AIP Journal of Applied Physics

Composition dependence of electronic structure and optical properties of Hf 1 x Si x O y gate dielectrics

G. He, L. D. Zhang, G. W. Meng, G. H. Li, G. T. Fei, X. J. Wang, J. P. Zhang, M. Liu, Q. Fang, and Ian W. Boyd

Citation: Journal of Applied Physics **104**, 104116 (2008); doi: 10.1063/1.3029664

View online: http://dx.doi.org/10.1063/1.3029664

View Table of Contents: http://scitation.aip.org/content/aip/journal/jap/104/10?ver=pdfcov

Published by the AIP Publishing

Composition dependence of electronic structure and optical properties of $Hf_{1-x}Si_xO_y$ gate dielectrics

G. He,[1,a)] L. D. Zhang,[1] G. W. Meng,[1] G. H. Li,[1] G. T. Fei,[1] X. J. Wang,[1] J. P. Zhang,[1] M. Liu,[1] Q. Fang,[2,b)] and Ian W. Boyd[2]
[1]*Key Laboratory of Materials Physics and Anhui Key Laboratory of Nanomaterials and Nanostructure, Institute of Solid State Physics, Chinese Academy of Sciences, Hefei 230031, China*
[2]*London Centre for Nanotechnology and Electronic and Electrical Engineering, University College London, Torrington Place, London WC1E 7JE, United Kingdom*

(Received 14 July 2008; accepted 9 October 2008; published online 24 November 2008)

Composition-dependent electronic structure and optical properties of $Hf_{1-x}Si_xO_y$ ($0.1 \leq x \leq 0.6$) gate dielectrics on Si at 450 °C grown by UV-photo-induced chemical vapor deposition (UV-CVD) have been investigated via x-ray photoemission spectroscopy and spectroscopy ellipsometry (SE). By means of the chemical shifts in the Hf 4*f*, Si 2*p*, and O 1*s* spectra, the Hf–O–Si bondings in the as-deposited films have been confirmed. Analyses of composition-dependent band alignment of $Hf_{1-x}Si_xO_y$/Si gate stacks have shown that the valence band (VB) offset (ΔE_v) demonstrates little change; however, the values of conduction band offset (ΔE_c) increase with the increase in the silicon atomic composition, resulting from the increase in the separation between oxygen 2*p* orbital VB state and antibonding *d* states intermixed of Hf and Si. Analysis by SE, based on the Tauc–Lorentz model, has indicated that decreases in the optical dielectric constant and increase in band gap have been observed as a function of silicon contents. Changes in the complex dielectric functions and band gap E_g related to the silicon concentration in the films are discussed systematically. From the band offset and band gap viewpoint, these results suggest that $Hf_{1-x}Si_xO_y$ films provide sufficient tunneling barriers for electrons and holes, making them promising candidates as alternative gate dielectrics. © *2008 American Institute of Physics*. [DOI: 10.1063/1.3029664]

I. INTRODUCTION

HfO_2-based gate dielectrics have a high potential for the next generation of ultralarge-scale integration device applications as alternatives to conventional SiO_2, which suffers from excess direct tunneling leakage currents resulting from the downscaling of complementary metal-oxide semiconductor field effect transistors.[1] Compatibility of the gate dielectrics with current device processing is mainly determined by a trade-off between high dielectric constant (high-*k*) and thermal stability. Although HfO_2 has been paid more attention recently, there still remain some problems to be solved such as the low crystallization temperature and the low immunity to oxygen.[2–5] Currently, several investigations have indicated that SiO_2 doped HfO_2 results in a significant improvement in electric properties as well as in thermal stability.[6–8] Furthermore, Hf-silicate films can further avoid the formation of low-*k* interfacial oxide layers due to a high resistivity to oxygen diffusion. On the other hand, the incorporation of SiO_2 into HfO_2 helps for stabilizing an amorphous Hf-silicate structure during high-temperature annealing. Therefore, Hf silicate is thus regarded as a promising candidate in direct contact with Si.[1,7,9]

Although there have been reports on the interface thermal stability and electrical properties,[1,7] the composition-dependent optical properties and electronic structure of $Hf_{1-x}Si_xO_y$/Si gate stacks have not been systematically investigated. Therefore, for understanding the effect of composition on the electrical performance of the Hf-silicate dielectric films, the chemical states and optical properties of $Hf_{1-x}Si_xO_y$/Si gate stacks should be determined explicitly. Since accurate determination of the optical properties is an essential prerequisite for device simulations and gives the opportunity to improve material preparation, this necessitates the investigation of optical characteristics for $Hf_{1-x}Si_xO_y$ thin films in the wide energy range. Recently, it has been noted that two processing methods, such as atomic layer deposition and metal organic chemical vapor deposition (MOCVD), have been paid much attention.[10–12] These two methods have major advantages of high film uniformity and superior conformal step coverage. A variety of precursor combinations have been investigated, for instance $(HfO_2)_{1-x}(SiO_2)_x$ has been deposited by liquid injection MOCVD using $[Hf(NEt_2)_4]$ in combination with $[Si(NMe_2)_4]$.[13] The combination of metal alkylamide $[Hf(NR_2)_4]$ and alkoxy silanol $[(RO)_3SiOH]$ sources have been proposed as a general method for the CVD of Hf silicate.[14] However, there have been few reports on the fabrication and physical properties of $Hf_{1-x}Si_xO_y$ gate dielectrics by new-typed UV-photo-induced CVD (UV-CVD) method.

The deposition of thin $Hf_{1-x}Si_xO_y$ films on Si by photo-induced CVD (photo-CVD) using UV excimer lamps at temperatures of 450 °C has been investigated in this letter. The advantage of UV-photo-assisted CVD processes is the use of the relatively high intensity of ultraviolet radiation to enable the initiation of photochemical reaction pathways leading to

a)Author to whom correspondence should be addressed. Electronic mail: ganghe01@issp.ac.cn.
b)Present address: Oxford Instruments, North End, Bristol BS49 4AP, United Kingdom.

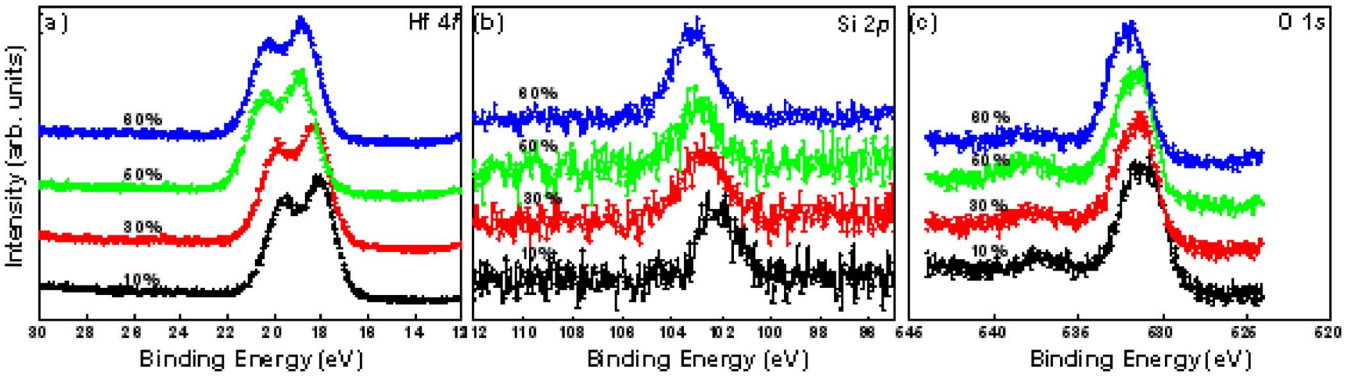

FIG. 1. (Color online) XPS of composition dependence in Hf 4*f* (a), Si 2*p* (b), and O 1*s* (c) photoemission spectra for the $Hf_{1-x}Si_xO_y$ films.

deposition, which are not accessible by thermal processing and generally lead to low thermal activation energy CVD processes. The excimer UV-lamp assisted photo-CVD technique is well established for the fabrication of high-*k* gate dielectrics in our previous work.[15,16]

In this letter, we obtained high-quality $Hf_{1-x}Si_xO_y/Si$ gate stacks at 450 °C by UV-CVD. By means of characterization from x-ray photoelectron spectroscopy (XPS) and spectroscopic ellipsometry (SE), the chemical bonding states, electronic structure, optical properties, and band alignments of $Hf_{1-x}Si_xO_y/Si$ gate stacks as a function of silicon content have been investigated in detail.

II. EXPERIMENTAL DETAILS

$Hf_{1-x}Si_xO_y$ thin films were grown by photo-CVD using an excimer lamp emitting 222 nm radiation at a growth temperature of 450 °C on Si wafers. Hafnium(IV) bis-*t*-butoxide-(bis)1-methoxy-2-methyl-2-propoxide, $Hf(OBu^t)_2(mmp)_2$ (made by Epichem, UK) and tetraethoxysilane $Si(OC_2H_5)_4$ (Aldrich, UK) were chosen as the precursor. N_2O was chosen to act as the oxidant. Prior to growing the hafnium silicate film, the Si wafers were precleaned by a standard RCA processing, then the wafers were immersed in a dilute hydrofluoric acid (HF, 1%) solution for 2–5 s to remove native oxide and the silicon dangling bonds passivated with hydrogen atom, followed by a de-ionized water rinsing. $Hf_{1-x}Si_xO_y$ films with different compositions were obtained by adjusting the atomic ratio of Si/(Hf+Si). Four groups of $Hf_{1-x}Si_xO_y$ samples with 10% Si (S1), 30% (S2), 50% (S3), and 60% (S4) were prepared. Details of the UV-CVD-derived $Hf_{1-x}Si_xO_y$ gate dielectrics have been described elsewhere.[17] The chemical bonding states and band alignments of the targeted $Hf_{1-x}Si_xO_y$ films on Si have been investigated by *ex-situ* XPS (ESCALAB MK2) system, equipped with an Mg $K\alpha$ radiation source (1253.6 eV) and hemispherical analyzer with a pass energy of 20 eV. The collected data were corrected for charging effect-induced peak shifts using the binding energy (BE) of adventitious carbon C 1*s* peak (284.6 eV). The intensities for all the XPS spectra reported here have been normalized for comparison. An *ex-situ* phase modulated SE (UVISEL Jobin-Yvon) measurement was performed with a spectral range of 0.75–6.5 eV in steps of 50 meV at room temperature. By spectroscopic spectra analysis based on the accurately parametrized Tauc–Lorentz (TL) dispersion relation for the $Hf_{1-x}Si_xO_y$ films, the thickness and the optical properties of the $Hf_{1-x}Si_xO_y$ films related to different atomic compositions have been obtained.

III. RESULTS AND DISCUSSION

A. XPS characterization

Figure 1 illustrates the silicon composition dependence of Hf 4*f* and Si 2*p* core-level spectra for the $Hf_{1-x}Si_xO_y$ films. For sample S1, the binding energies corresponding to Hf $4f_{7/2}$ to Hf $4f_{5/2}$ are located at 18.2 and 19.6 eV, respectively. Compared to our reported values of 17.3 and 18.9 eV for Hf $4f_{7/2}$ and Hf $4f_{5/2}$ peaks of HfO_2,[4] there is a shift (~1 eV) of the Hf $4f_{7/2}$ peak for sample S1 toward a higher BE, which implies the change in the Hf chemical environment. It has been reported that the Hf 4*f* electron peaks in hafnium silicate appear at 18.2 and 19.7 eV, about 1.0 eV higher than those in HfO_2.[1] It confirms that sample S1 has silicate structure. Another important feature of S1 sample tested shows no evidence of the Hf 4*f* electron peaks associated with Hf–Si bonds located at 14.3 and 15.8 eV.[1] This means that the present sample has no silicide bonds and that the Si and Hf atoms form chemical bonds solely with O atoms. The lack of Hf–Si bonding is expected because deleterious Hf–Si bonding will be energetically unfavorable compared to Si–O bonds at the interface. With the increase in the atom ratio of Si/(Hf+Si) in the precursor solution, it can be clearly seen that the two peaks of Hf 4*f* electrons show a slight shift toward higher BE side, which is in good agreement with the observation of Kato *et al.*[18] A similar shift in photoemission BE with composition of Hf silicate has also been suggested by Opila *et al.*[19] In all cases, the BE of the Hf 4*f* is greater for the silicate than for the pure HfO_2, reaching a shift of 1.2 eV for sample S4. According to the conclusion of Opila *et al.*,[19] the BE shift can be due to the relatively less electron-donating nature of the second-nearest-neighbor silicon relative to hafnium. The decreased electron donation from the second-nearest neighbor increases the initial state energy of the metal electron by slightly decreasing the electron density on the metal atom. Less electron density reduces the screening of the metal core level, thereby increasing the measured BE. In addition, the decreased electron donation from the Si destabilizes the photoemission final state located

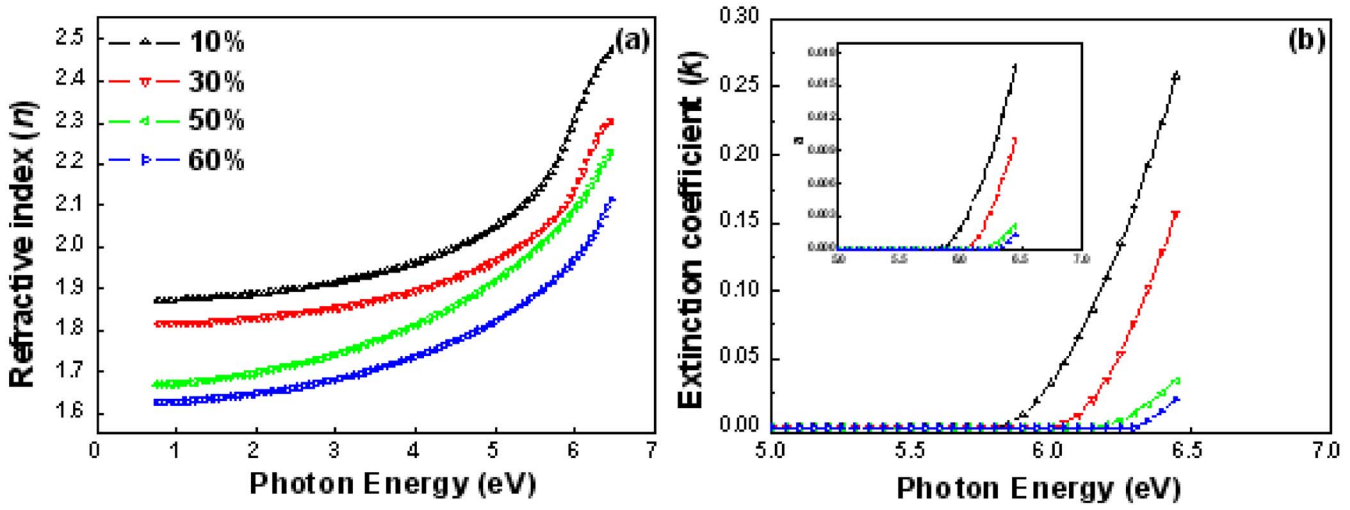

FIG. 2. (Color online) The composition-dependence of refractive index (n) and extinction coefficient (k) of the $Hf_{1-x}Si_xO_y$ films. The inset in (b) is the composition-dependence curves of the absorption coefficient.

on the metal since the slightly decreased electron density on the metal atom results in the decreased screening of the final state ion.

As shown in Fig. 1(b), The Si 2p peaks, centered at around 102–102.7 eV, can originate from the Hf-silicate film, and they are associated with Hf–O–Si bonds.[10] With the increase in the Si content in the films, the Si 2p core-level spectra shift monotonically to a higher BE side with the increase in the Si atomic ratio. Taking all results into consideration, this chemical shift is believed to be reflection of the difference in the second-nearest atoms around the Si atoms. Compared to the pure SiO_2, all the Si core-level spectra demonstrate apparent shifts toward lower BEs, suggesting the formation of the Hf–Si–O bonds in the films.

To gain further insights into the transition of the chemical bonding states of the $Hf_{1-x}Si_xO_y$ layers related to the different Si compositions, XPS spectra for the O 1s have also been investigated. As shown in Fig. 1(c), all the BEs of O 1s peaks locate at between our previous reported HfO_2 and SiO_2 and shift to a BE with an increase in the silicon atomic ratio. Meanwhile, their full widths at half maximum increase correspondingly, supportive of the view that all the samples are composed of Si–O and Hf–O bonds. Since the shifts of the Si 2p and metal core-level BE vary continuously with silicon composition, it can be inferred that the silicate composition can be deduced from the peak shift of the XPS spectra.

B. Optical properties

An *ex-situ* phase modulated SE (UVISEL Jobin-Yvon) was used to measure the optical functions of $Hf_{1-x}Si_xO_y$ films with different silicon contents at room temperature in the spectral range of 0.75–6.5 eV with a step of 50 meV at an incident angle of 70°. In order to determine the optical properties of $Hf_{1-x}Si_xO_y$ films with different atomic compositions, a TL dispersion function has been adopted to investigate the optical dielectric functions of the $Hf_{1-x}Si_xO_y$ films.[20,21] Essentially, the imaginary part (ε_2) of dielectric functions is obtained by combining the classical expression of the imaginary part of the dielectric functions above the band edge and the standard Lorentz expression, and the real part (ε_1) of dielectric functions is the result of self-consistent Kramers–Kronig integration of ε_2. The following equations summarize ε_1 and ε_2 as a function of photon energy E:

$$\varepsilon_2(E) = \begin{cases} \dfrac{AE_0C(E-E_g)^2}{(E^2-E_0^2)^2+C^2E^2}\dfrac{1}{E} & (E > E_g) \\ 0 & (E \le E_g) \end{cases} \quad (1)$$

and

$$\varepsilon_1(E) = \varepsilon_\infty + \frac{2P}{\pi}\oint \frac{\xi\varepsilon_2(\xi)}{\xi^2-E^2}d\xi. \quad (2)$$

Equations (1) and (2) are uniquely defined by four parameters A (transition matrix element), C (broading term), E_0 (peak transition energy), and E_g (optical band gap). All the fitted parameters from SE have a confidence limit better than 90%.

Figure 2 presents the dispersion curves of refractive index (n) and extinction coefficient (k) of $Hf_{1-x}Si_xO_y$ films as determined by SE. It can be observed that the refractive index decreases with the increase in Si concentration in the films. According to Lorentz–Lorentz relation,[22] it has been seen that the refractive index can be related to the evolution of packing density and polarizability. Due to the incorporation of silicon content, such a substitution in the anion lattice to hafnium holds the promise to decrease the refractive index since Si–O bonds tend to be less polar than the corresponding Hf–O bonds, leading to a lower polarizability. With the increase in silicon content in the films, lower polarizabilty leads to the lowering of the refractive index.

As shown in Fig. 2(b), the extinction coefficient for all the samples saturates to zero in the visible region, suggesting the realization of high-quality $Hf_{1-x}Si_xO_y$ film in terms of optical properties. An abrupt increase in the extinction coefficient for higher photon energy, attributed to the defect density in the films, has been observed, indicating fundamental band gap absorption in the films. In the inset of the Fig. 2(b), the dependence curves of absorption coefficient (α

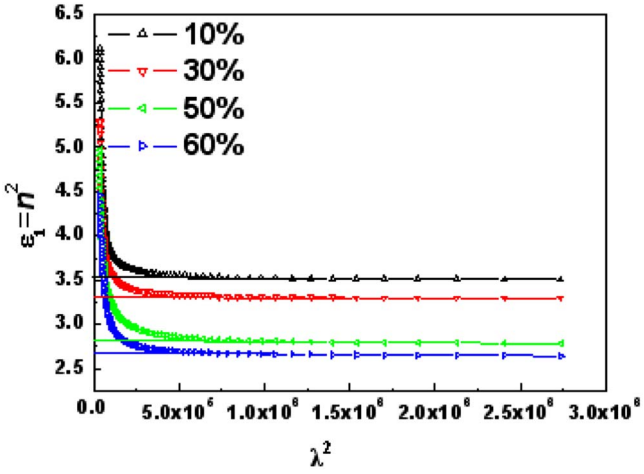

FIG. 3. (Color online) Plots of ε_1 as a function of λ^2 for the $Hf_{1-x}Si_xO_y$ films.

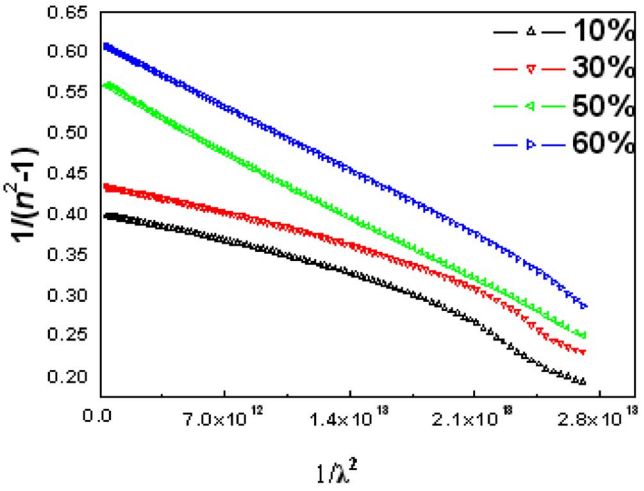

FIG. 4. (Color online) Plots of $1/n^2-1$ vs $1/\lambda^2$ for the $Hf_{1-x}Si_xO_y$ films.

$=4\pi k/\lambda$) near the band edge of all the samples are displayed. It has been found that the shape of the curves is similar to that of the extinction coefficient. With the increase in the silicon composition in the films, the absorption band edge continues to shift toward the higher energy side, which is consistent with PECVD-derived Hf-silicate films.[18] As we know, a shift in the optical absorption band edge corresponds to a change in the band gap.[23] So the evolution of the band gap related to the silicon composition will be explained in detail below.

1. Determination of high frequency dielectric constant

The resultant data of the refractive index can be analyzed to obtain the high frequency dielectric constant via two procedures. The first procedure describes the contribution of the free carriers and the lattice vibration modes of the dispersion. The second procedure is based on the dispersion resulting from the bound carriers in an empty lattice. In order to obtain a reliable value for the high frequency dielectric constant ε_∞, both procedures have been employed.

a. The first procedure The high frequency dielectric constant can be obtained by following equation:[24]

$$\varepsilon_1 = \varepsilon_{\infty(1)} - B\lambda^2 \tag{3}$$

where ε_1 is the real part of dielectric constant, $\varepsilon_{\infty(1)}$ is the lattice dielectric constant (high frequency dielectric constant), and λ is the wavelength. The real part of dielectric constants $\varepsilon_1=n^2$ was calculated at different values of λ. Then, the obtained values of ε_1 are plotted as a function of λ^2 as shown in Fig. 3. It has been observed that the dependence of ε_1 on λ^2 is linear at longer wavelength. Extrapolating the linear part of this dependence to zero wavelength produces the value of $\varepsilon_{\infty(1)}$, given in Table I.

b. The second procedure The high frequency dielectric constant can be calculated by applying the following simple classical dispersion relation:[25]

$$(n^2-1) = \left[\frac{S_0\lambda_0^2}{1-(\lambda^2/\lambda_0^2)}\right], \tag{4}$$

$$S_0 = \frac{(n_0^2-1)}{\lambda_0^2}, \tag{5}$$

where λ_0 is an average oscillator position, S_0 is an average oscillator strength, and n_0 is the refractive index at infinite wavelength λ_0 (average interband-oscillator wavelength). The plots of $1/n^2-1$ versus $1/\lambda^2$ give straight lines with different slopes and fit the classical dispersion formula with a single electronic oscillator well, as shown in Fig. 4. The parameters S_0 and λ_0 can be deduced from the slope $(-1/S_0)$ of the resulting straight line and the infinite wavelength intercept $(1/S_0\lambda_0^2)$, respectively. The average interband-oscillator energy can be given by $E_0=hc/\lambda_0$, where h is Planck's constant and c is the velocity of light. The refractive index dispersion parameter (E_0/S_0) and the high frequency dielectric constant $\varepsilon_{\infty(2)}=n_0^2$, which depends on the characteristics of the various interband transitions, can also be determined, shown in Table I. From Table I, it can be noted that the values of $\varepsilon_{\infty(1)}$ and $\varepsilon_{\infty(2)}$ obtained from the two

TABLE I. Dispersion parameters of the as-deposited $Hf_{1-x}Si_xO_y$ films with different silicon concentrations. The estimated precision is 10% for these values.

Samples	Si concentration (at. %)	S_0 (m^{-2})	λ_0 (nm)	E_0 (eV)	E_0/S_0	ε_∞ (1)	ε_∞ (2)
S1	10	1.73×10^{14}	120	10.35	5.98×10^{-14}	3.53	3.50
S2	30	1.64×10^{14}	117	10.61	6.47×10^{-14}	3.30	3.27
S3	50	0.91×10^{14}	140	8.87	9.74×10^{-14}	2.79	2.78
S4	60	0.84×10^{14}	139	8.93	10.63×10^{-14}	2.65	2.64

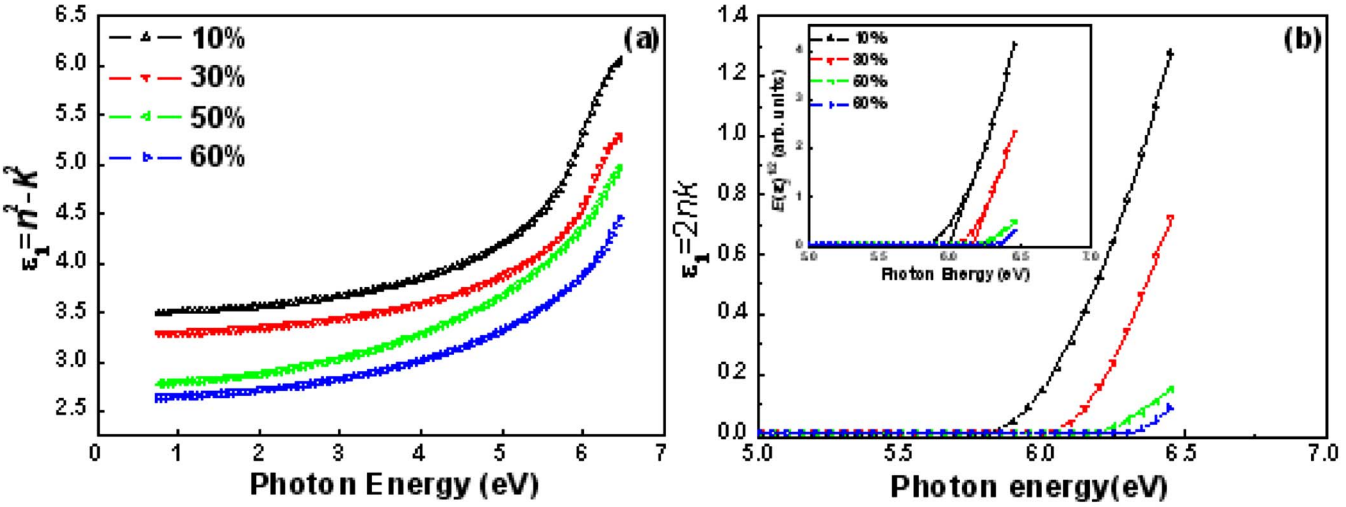

FIG. 5. (Color online) The real and imaginary parts of the pseudodielectric functions $\varepsilon=\varepsilon_1+i\varepsilon_2$ of the as-deposited $Hf_{1-x}Si_xO_y$ films calculated from the SE fitting. The inset in (b) is the determination of the optical band gap of the $Hf_{1-x}Si_xO_y$ films.

procedures approximately agreed with each other may be attributed to the lattice vibrations. What's more, with the increase in the silicon concentration in the films, the high frequency dielectric constants decrease, which will be discussed later.

2. Determination of complex dielectric constant

The complex refractive index $n=n+ik$ and dielectric function $\varepsilon_1=\varepsilon_1+i\varepsilon_2$ characterize the optical properties of any solid material. The imaginary and real parts of dielectric constant of thin films were also determined by the following relations:[26]

$$\varepsilon_1 = n^2 - k^2, \quad \varepsilon_2 = 2nk.$$

Figure 5(a) shows the atomic composition dependence of the real (ε_1) part (optical dielectric constants) of the optical dielectric function of $Hf_{1-x}Si_xO_y$ films as determined by SE. It can be seen that ε_1 decreases with the increase in the silicon atomic composition. It has been reported that the optical dielectric constants decrease with the increase in the band gap energy, which is due to the fact that the optical dielectric constant originating from electronic polarizability is strongly dependent on the width of the band gap energy and is nearly independent of the origin of the band gap, i.e., the atomic composition.[27] This result suggests that the evolution of the optical dielectric constants is attributed to the change in the optical band gap with the increase in the silicon atomic composition.

Figure 5(b) presents the spectra of the imaginary (ε_2) part of the dielectric functions for samples S1, S2, S3, and S4. From the plots, it can be observed that the dielectric functions for all the samples are the same in the transparent region, but different in the absorption region, originating from the atomic composition-deduced structure change. According to the previous report,[28] the optical band gap can be obtained from the imaginary part of the dielectric constant $\varepsilon_2=2nk$. The inset in Fig. 3(b) illustrates a plotting of $(E)^2\varepsilon_2^{1/2}$ against $h\nu$. The linear part of this graph is described by the following relation:[29]

$$E^2\varepsilon_2 = (h\nu - E_g)^2.$$

The optical band gap values extracted by extrapolating the straight near the band edge to zero are 5.99, 6.14, 6.24, and 6.35 eV for samples S1, S2, S3, and S4, respectively, demonstrating that the band gap gradually increases with the increase in the silicon atomic composition from 10% to 60%. Similar experimental results have also been found in the PECVD-derived Hf-silicate films.[18] Compared to pure SiO_2, a decreased band gap in Hf silicate has been observed. It is known that the nonbonding O $2p$ states form the top of the valence SiO_2 and that the Si–O antibonding states form the bottom of its conduction band (CB).[30] In the case of $Hf_{1-x}Si_xO_y$ nonbonding O $2p$ states form the top of the valence band (VB) and the antibonding d states of hafnium form the lowest CB states. The localized d states locate below the CB minimum of SiO_2. The localized d states do not mix significantly with the extended s-like CB states of the SiO_2 host oxide, attributing a decreased band gap. With the increase in the silicon atomic composition, it is believed that the intermixing of these two oxides, with SiO_2 having a larger band gap, increases the separation of the oxygen $2p$ orbital VB state and the antibonding d states intermixed of Hf and Si, and therefore results in the increase in the band gap.

Band offsets are a strong constraint on the choice of high-k as both the CB and VB offsets must be over 1 eV to act as sufficient injection barriers. In all high-k oxides of interest, the CB offset is much less than the VB offset and is the main constraint. Therefore, it is necessary to investigate the evolution of the CB offset of $Hf_xSi_{1-x}O/Si$ gate stack. Based on the method proposed by Kraut *et al.*,[31] the VB alignment of $Hf_{1-x}Si_xO_y$ films on the Si substrate could be determined by measuring the VB maximum (E_v) difference between the $Hf_{1-x}Si_xO_y$ films and the H-terminated Si substrate, as expressed in the following equation:

$$\Delta E_v(Hf_{1-x}Si_xO_y - Si) = E_v(Hf_{1-x}Si_xO_y) - E_v(Si).$$

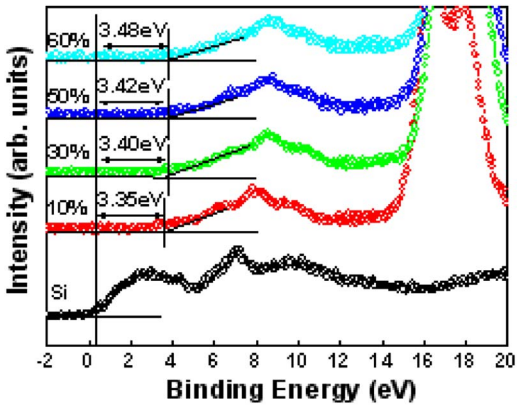

FIG. 6. (Color online) Composition dependence in valence band photoemission spectra of $Hf_{1-x}Si_xO_y$/Si gate stacks.

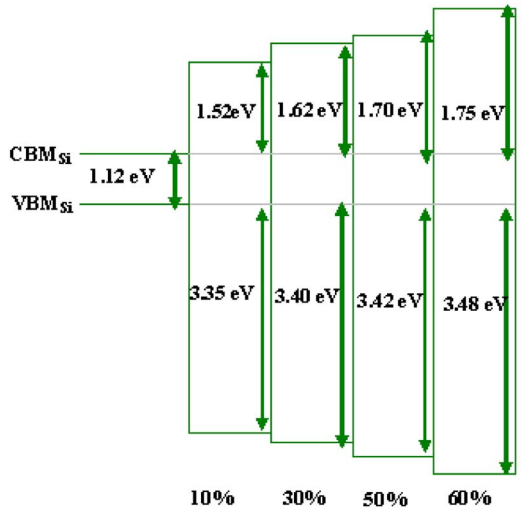

FIG. 7. (Color online) Schematic band diagram of $Hf_{1-x}Si_xO_y$/Si gate stacks with different Si compositions.

Here, E_v is determined by extrapolating the leading edge of the VB spectrum to the baseline, the crossing point is taken to be E_v, as shown in Fig. 6. The leading edge of VB spectrum for *p*-type Si substrate used in this work was at 0.30 eV in our measurement. Therefore, ΔE_v values of 3.35, 3.40, 3.42, and 3.48 are obtained for samples S1, S2, S3, and S4, respectively. It is obvious that the VB offset shows little change with the increase in the silicon atomic composition due to the interaction of the nonbonding Hf 5*d* states with the adjacent O. Compared to that of pure HfO_2 thin film,[32] the leading edges of VB spectra of $Hf_{1-x}Si_xO_y$ demonstrate an obvious redshift. Similar to the case of HfO_2, the O *p* states form the VB, while the Hf *d* states form the CB of $Hf_{1-x}Si_xO_y$. The major difference between HfO_2 and $Hf_xSi_{1-x}O$ stems from the extent of mixing of the VB between Hf *d* and O *p*, which indirectly correlates to the ionic/covalence behavior of the materials. In this case $Hf_{1-x}Si_xO_y$ shows a more covalence behavior than HfO_2, attributing the reduced VB edge. According to our results, it can be concluded that the VB offset of $Hf_{1-x}Si_xO_y$ film relative to Si is in the range of 3.35–3.48 eV, which is similar to the reported values.[10]

From the values of VB offsets and band gap determined above, the CB offset $\Delta E_c(Hf_{1-x}Si_xO_y-Si)$ between $Hf_{1-x}Si_xO_y$ and Si can be obtained through the expression

$$\Delta E_c(Hf_{1-x}Si_xO_y - Si) = E_g(Hf_{1-x}Si_xO_y) - \Delta E_v(Hf_{1-x}Si_xO_y - Si) - E_g(Si).$$

ΔE_c values of the $Hf_{1-x}Si_xO_y$ films with different silicon atomic compositions are calculated as 1.52, 1.62, 1.70, and 1.75 eV, respectively. Figure 7 shows a summary of the schematic band diagram of $Hf_{1-x}Si_xO_y$ gate dielectrics with different compositions. According to our previous reported ΔE_c value of pure HfO_2,[33] it can be noted that the CB offsets demonstrate an apparent increase with the increase in the silicon atomic composition. This can be explained that the CB minimum is mainly due to nonbonding Hf 5*d* states and also lies at a fixed energy. With the increase in silicon atomic composition, the increase in the separation between the oxygen 2*p* orbital VB state and the antibonding *d* states intermixed of Hf and Si brings about the increase in CB offset. These results suggest that $Hf_{1-x}Si_xO_y$ dielectric films provide sufficient tunneling barriers for both of electrons and holes, making them suitable candidates as alternative gate dielectrics.

IV. CONCLUSION

In summary, the electronic structure, band alignments, and optical properties of $Hf_{1-x}Si_xO_y$ gate dielectrics on Si substrate, grown by UV-CVD, have been investigated as a function of silicon contents. XPS measurements have confirmed that the as-deposited films grown by UV-CVD are Hf silicate with Hf–Si–O bonds and no Hf–Si bonds are found. According to the analyses of composition-dependent band alignments of $Hf_{1-x}Si_xO_y$/Si gate stacks, an increase in CB offset as well as band gap has been observed but only little change for VB offsets of $Hf_{1-x}Si_xO_y$ films, originating from the increase in the separation between the oxygen 2*p* orbital VB state and the antibonding *d* states intermixed of Hf and Si with the increase in silicon contents. Characterization from SE, based on the TL model, has indicated that decreases in the optical dielectric constants and increase in band gap have been observed as a function of silicon contents. From the band offset viewpoint, the suitable band gap and band offsets relative to Si make UV-CVD-derived $Hf_{1-x}Si_xO_y$ film as a promising candidate for high-*k* gate dielectrics.

ACKNOWLEDGMENTS

This work was supported by the National Natural Science Foundation of China (Grant Nos. 10804109 and 10674138) and Royal Society U.K. (Grant No. IJP-2006/R1).

[1]G. D. Wilk, R. M. Wallace, and J. M. Anthony, J. Appl. Phys. **89**, 5243 (2001).
[2]W. Zhu, T. P. Ma, T. Tamagawa, Y. Di, J. Kim, R. Carruthers, M. Gibso, and T. Furukawa, Tech. Dig. - Int. Electron Devices Meet. **2001**, 20.4.1.
[3]C. H. Choi, S. J. Rhee, T. S. Jeon, N. Lu, J. H. Sim, R. Clark, M. Niwa, and D. L. Kwang, Tech. Dig. - Int. Electron Devices Meet. **2002**, 865.
[4]G. He, M. Liu, L. Q. Zhu, M. Chang, Q. Fang, and L. D. Zhang, Surf. Sci. **576**, 67 (2005).
[5]G. He, Q. Fang, M. Liu, L. Q. Zhu, and L. D. Zhang, J. Cryst. Growth

268, 155 (2004).
[6]D. A. Neumayer and E. Cartier, J. Appl. Phys. **90**, 1801 (2001).
[7]G. D. Wilk and R. M. Wallace, Appl. Phys. Lett. **74**, 2854 (1999).
[8]G. He, L. D. Zhang, and Q. Fang, J. Appl. Phys. **100**, 083517 (2006).
[9]M. Ritala, K. Kukli, A. Rahtu, P. I. Räisänen, M. Leskelä, T. Sajavaara, and J. Keionen, Science **288**, 319 (2000).
[10]H. Jin, S. K. Oh, H. J. Kang, and M.-H. Cho, Appl. Phys. Lett. **89**, 12290 (2006).
[11]R. Ludeke and E. Gusev, J. Appl. Phys. **96**, 2365 (2004).
[12]Y. Xuan, D. Hojo, and T. Yasuda, Appl. Phys. Lett. **84**, 5097 (2004).
[13]B. C. Hendrix, A. S. Borovik, C. Xu, J. F. Roeder, T. H. Baum, M. J. Bevan, M. R. Visokay, J. J. Chambers, A. L. P. Rotondaro, H. Bu, and L. Colombo, Appl. Phys. Lett. **80**, 2362 (2002).
[14]R. G. Gordon, J. Becker, D. Hausmann, and S. Suh, Chem. Mater. **13**, 2463 (2001).
[15]Z. M. Wang, Q. Fang, J.-Y. Zhang, J. X. Wu, Y. Di, W. Chen, and I. W. Boyd, Thin Solid Films **453–454**, 167 (2004).
[16]Q. Fang, J. Y. Zhang, Z. M. Wang, G. He, and I. W. Boyd, Microelectron. Eng. **66**, 621 (2003).
[17]M. Liu, L. Q. Zhu, G. He, Z. M. Wang, J. X. Wu, J. Y. Zhang, I. Liaw, Q. Fang, and I. W. Boyd, Appl. Surf. Sci. **253**, 7869 (2007).
[18]H. Kato, T. Nango, T. Miyagawa, T. Katagiri, K. S. Seol, and Y. Ohki, J. Appl. Phys. **92**, 1106 (2002).
[19]R. L. Opila, G. D. Wilk, M. A. Alam, R. B. van Dover, and B. W. Busch, Appl. Phys. Lett. **81**, 1788 (2002).
[20]G. He, L. D. Zhang, G. H. Li, M. Liu, L. Q. Zhu, S. S. Pan, and Q. Fang, Appl. Phys. Lett. **86**, 232901 (2005).
[21]G. He, L. D. Zhang, G. W. Meng, G. H. Li, Q. Fang, and J. P. Zhang, J. Appl. Phys. **102**, 094103 (2007).
[22]D. Mergel, D. Buschendorf, S. Eggert, R. Grammes, and B. Samset, Thin Solid Films **371**, 218 (2000).
[23]R. Asahi, T. Morikawa, T. Ohwaki, K. Aoki, and Y. Taga, Science **293**, 269 (2001).
[24]J. N. Zemel, J. D. Jensen, and R. B. Schoolar, Phys. Rev. **140**, 330 (1965).
[25]F. Yakuphanoglu, A. Cukurovali, and I. Yilmaz, Physica B **351**, 53 (2004).
[26]M. M. Wakkad, E. Kh. Shokr, and S. H. Mohammed, J. Non-Cryst. Solids **265**, 157 (2000).
[27]M. Koike, T. Ino, Y. Kamimuta, M. Koyama, Y. Kamata, M. Suzuki, Y. Mitani, and A. Nishiyama, Phys. Rev. B **73**, 125123 (2006).
[28]P. Y. Yu and M. Cardona, *Fundamentals of Semiconductors* (Springer, Berlin, 2001), p. 259.
[29]K. Hukari, R. Dannenberg, and E. A. Stach, J. Mater. Res. **17**, 550 (2002).
[30]D. L. Griscom, J. Non-Cryst. Solids **24**, 155 (1977).
[31]E. A. Kraut, R. W. Grant, J. R. Waldrop, and S. P. Kowalczyk, Phys. Rev. Lett. **44**, 1620 (1980).
[32]J. Wang, J. W. Chai, Y. F. Dong, Y. P. Feng, N. Sutanto, J. S. Pan, and A. C. H. Huan, Appl. Phys. Lett. **88**, 192103 (2006).
[33]X. J. Wang, L. D. Zhang, M. Liu, J. P. Zhang, and G. He, Appl. Phys. Lett. **92**, 122901 (2008).